

Position Control of lower exoskeleton Rehabilitation system Based on an Optimized FADRC Controller

nasir alawad (✉ cse.20.33@grad.uotechnology.edu.iq)

Mustansiriyah University Faculty of Engineering <https://orcid.org/0000-0003-3059-4375>

AMJAD HUMAIDI

University of Technology

AHMED ALARAJI

University of Technology

Research Article

Keywords: Exoskeleton device, ADRC, Extended state observer, trajectory tracking, Fractional calculus, exogenous disturbance

Posted Date: May 19th, 2022

DOI: <https://doi.org/10.21203/rs.3.rs-1502806/v1>

License:   This work is licensed under a Creative Commons Attribution 4.0 International License.

[Read Full License](#)

Position Control of lower exoskeleton Rehabilitation system Based on an Optimized FADRC Controller

NASIR A. ALAWAD^{1*}, AMJAD J. HUMAIDI², AHMED S. ALARAJI³

¹Computer Engineering, Al-Mustansiriyah University, Baghdad-IRAQ

²Control and System Engineering, University of Technology, Baghdad, IRAQ
Amjad.j.humaidi@uotechnology.edu.iq

³Computer Engineering, University of Technology, Baghdad, IRAQ
Ahmed.s.alaraji@uotechnology.edu.iq

*Corresponding Author: cse.20.33@grad.uotechnology.edu.iq

Abstract. A rehabilitation exoskeleton with physiotherapists in their everyday using routine is gradually becoming the normal case. The Active Disturbance Rejection Controller (ADRC) is used in this article to control the proper execution of fundamental limb rehabilitation trainings. The experiment is carried out on a flexible single joint exoskeleton model, whose behavior is similar to that of a real robotic rehabilitation equipment. In this study, we used two ADRC configurations and compared their robustness to external and internal disturbances with uncertainty in system parameters, these classical or linear (LADRC) and optimized fractional ADRC (FADRC). According to the root mean square error (R.M.S.E) as a performance index tool, the results reveal that (FADRC) appears to be better than (LADRC). Matlab and the Simulink tools were used to create all simulation results.

Keywords: Exoskeleton device, ADRC, Extended state observer, trajectory tracking, Fractional calculus, exogenous disturbance.

1. Introduction

Exoskeleton technologies have advanced to allow people with limited physical abilities to complement their mechanical strength. The majority of power assist control systems function by estimating an idea of the user's intended motion in real time^[1]. Performance tracking after training with these devices reinforces the patient's recovery, and a comparison of improvement on the measured values may be utilized to provide justification.

For advances in the area of artificial treatment of the knee joints, many control systems are being used and human assistance exoskeletons have been developed. When there is no disturbance in the system, proportional-derivative (PD) based control performs well^[2], but when there is a disturbance in the system, it performs poorly^[3]. Intelligent control methods^[4] necessitate a significant amount of work in terms of rule formulation and inference testing. The presence of disturbance causes sensitivity amplification, which necessitates the use of an accurate inverse dynamic model^[5]. In such situations, one option is to use strong control systems, which are conservative and address terrible scenarios there at expense of transitory reaction. In^[6] proposes a particle swarm optimization (PSO)-based active control rejected regulation for eliminating perturbations in locomotors path planning, which requires a high degree of parameter evaluations,

but it does have a significant processing costs. The Radial basis function network is utilized to adjust for the disturbance^[7]. Sliding mode control (SMC) may prevent versus errors and variable changes, however it can chatter due to interrupted transition^[8]. Computed-torque control^[9] is based on the system's particular device and that may need more control to adjust for model problems. (ADRC) method is proposed to tackle such modern control challenges. Han^[10] was the first to suggest the ADRC controller, which has numerous advantages. The popularity of ADRC in flight control^[11], process control^[12-13], motion control applications^[14-15], and many other domains^[16] can be seen in its progress and rapid deployment in industries during the previous three decades. In industries, its applicability as a substitute for proportional–integral–derivative is being identified (PID). ADRC is similar to PID, however it has better qualities. ADRC's technology is designed to provide better solutions by aggressively reducing all internally and externally uncertainties^[17]. All that is required for ADRC to work as a model-free controller is the process ordering and the approximate values of system parameters^[18]. This focuses on error instead of framework control strategy^[19] and will not require detailed framework or process - based information, i.e., a precise description of the process^[20]. In the field of lower leg recovery, automated machines, orthotic devices, exoskeletons, and prostheses are being created to aid patients with treatment focuses as well as other activities including such seating, having to stand, and so on. A linear extended state observer (LESO) driven ADRC just on lower leg actuator for the knee and hip was used as a reference for medical gait data.

Due to its growing popularity and accuracy, ADRC was used in a variety of robotic help people for monitoring tasks in latest years^[21]. The outputs for PID and ADRC are compared, and the results demonstrate that ADRC outperform PID for knee trajectories and in terms of errors experiments, also the results have demonstrated that ARDC is effective. ADRC deals with nonlinearities^[22]. Position monitoring, force and impedance control, bio signals based control, and adaptive control are some of the control systems used in rehabilitation^[23]. Position tracking was among the most basic control algorithms for robotic rehabilitation systems, in which the controller improves the repeatability and position precision of motion for the patient's recovery^[24]. Because ADRC's nonlinear structure^[10] restricts its applicability in the engineering area, a linear active disturbance rejection, or LADRC, was developed to simplify the structure and is now frequently used^[25]. Using the fractional calculus, the classical extended states observer (ESO) is generalized to a fractional order extended states observer (FESO) in FADRC^[26]. In regards of robustness and disturbance rejection capability, several studies demonstrate that fraction-order active disturbance rejection controller (FADRC) exceeds integer-order ADRC^[27-28]. Chen^[29] suggested a FADRC control system comprising of a proportional controller and a fraction-order ESO, which has apparent advantages over integer-order LADRC in terms of robustness against noisy environments and perturbation. In^[30] suggested an ADRC and fraction-order PID (FOPID) direct torque control technique for the hydro-turbine speed governor system which is load disturbance tolerant. Because the integer order ESO (IESO) has poor prediction ability for high-frequency disturbances. In^[26] presented a FADRC control technique based on a fraction-order ESO (FESO) to enhance the system in control's performance.

The remainder of this work is laid out as follows. The suggested limb-rehabilitation device is described in Section 2. The exoskeleton system is shown in Section 3 with various configurations

of the ADRC control approach. In Section 4, you can view the experimental results for various ADRC settings. Finally, in Section 5, the conclusion is presented, along with some additional views on future research on the subject at hand.

2. Exoskeleton Device Model

The human shank and the exoskeleton make up the system. The exoskeleton is a mechanical device that is custom-fit to the wearer's leg and is held in place by braces. The model consists of knee joint movement controlled by a single D.C motor embedded in the structure, and the entire system is in synchronized motion as illustrated in Fig.1. Table 1 lists the specifications of the exoskeleton^[31].

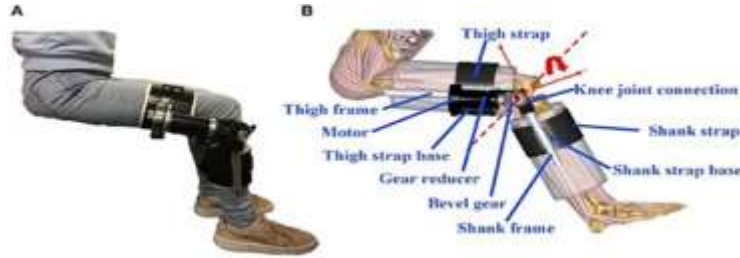


Fig. 1. (A) Knee exoskeleton prototype; (B) Mechanical and Electrical parts.

Table 1. Systems identified parameters^[31]

parameter	value
Inertia (J)	0.359 Kg.m ²
Solid Friction Coefficient (A)	1.026N.m
Viscous Friction Coefficient (B)	1 N.m.s./rad
Gravity Torque (τ_g)	3.218N.m

Generally the dynamic model of lower knee joint motion is^[31]:-

$$J\ddot{\theta} = -\tau_g \cos \theta - A \text{sign}\dot{\theta} - B\dot{\theta} + \tau_c + \tau_h \quad (1)$$

θ is the knee joint angle between the actual position of the shank and the full extension position, $\dot{\theta}$ and $\ddot{\theta}$ are respectively the knee joint angular velocity and acceleration. $J, A, B, \tau_g, \tau_c, \tau_h$ are Inertia, solid friction coefficient, viscous friction coefficient, gravity torque, controller torque and human torque respectively.

3. ADRC methodology

Three are three basic components of the ADRC are the tracking differentiator (TD), the extended state observer (ESO), and the linear state error feedback law (LSEF). The TD arranges the transition process and gives differential signal, the ESO collects the element's specialized output to evaluate the element's error change and noise. Finally, using the error between the general input and the general output to feed it to the LSEF and generates the control action to compensate any disturbance^[10]. Fig. 2. shows the structure using LADRC topology as applied to an exoskeleton system.

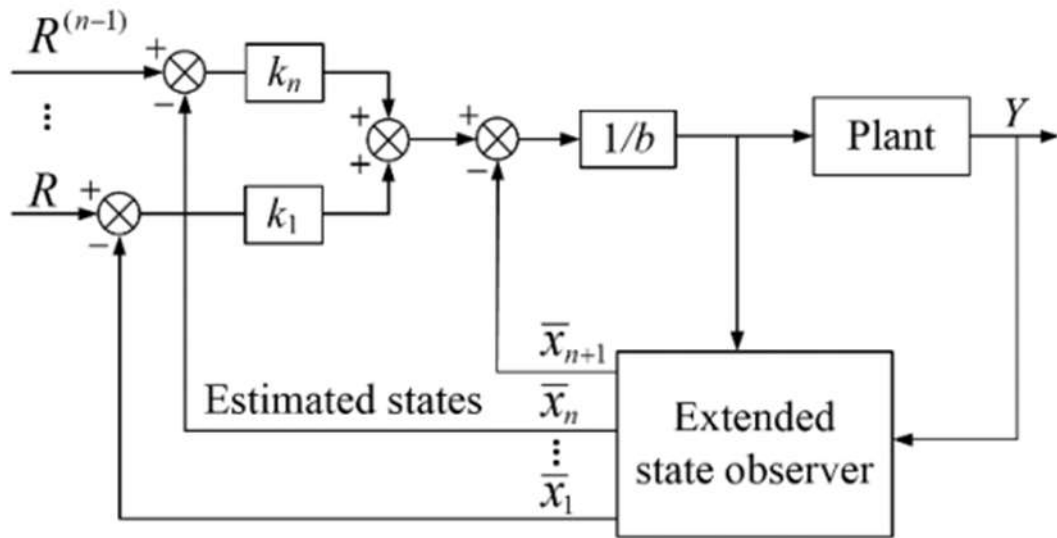


Fig. 2. General LADRC Structure

Finally, by changing the ESO to fractional ESO and reconstructing ADRC as FADRC, another configuration was created. Fig. 3. Shows only the fractional FESO .

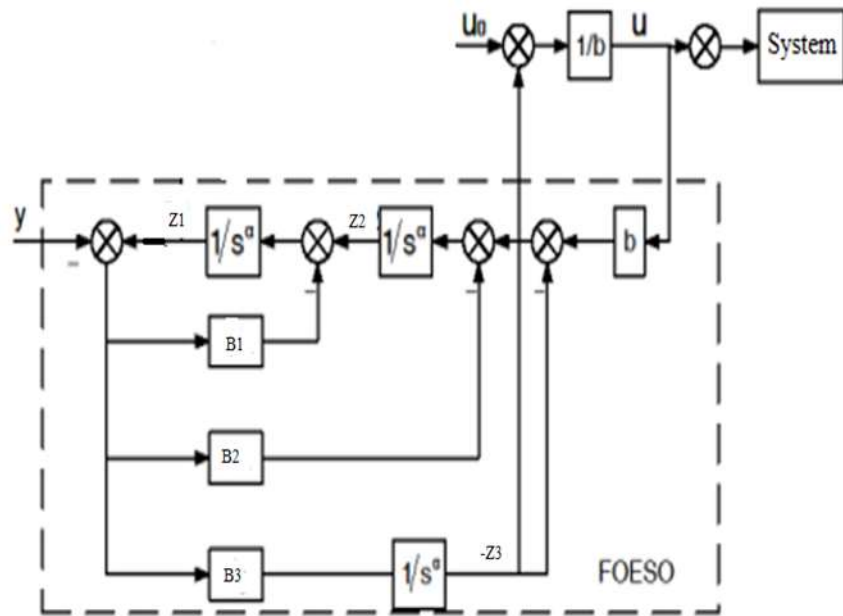


Fig. 3. FESO of FADRC Structure

3.1 Tracking Differentiator (TD)

To avoid overrun and maximize system performance, the TD is widely utilized. It uses a differential transitory characteristic of incoming signal to eliminate rapid changes, resulting in a

gradual increase in output rather than sudden increases, in this part using only the signal and its derivative(linear TD):-

$$\begin{aligned} v_1 &= R \\ v_2 &= \dot{R} \end{aligned} \quad (2)$$

3.2 Extended state observer (ESO)

In this work, using two types of ESO for comparison purpose:-

3.2.1 Linear ESO

The following is the nonlinear model for the controlled plant subjected to uncertain internally and externally disturbances^[32-33]:

$$\begin{cases} \dot{\psi}_1 = x_2 \\ \dot{\psi}_2 = f(\psi, w, t) + bu \\ y = \psi_1 \end{cases} \quad (3)$$

Where, u and y are the input and output signals, $f(\psi, w, t)$ is the unknown nonlinear system function including disturbance, and b is the control gain.

$\psi_3 = f(\psi, w, t) + \Delta bu$ is the new expanded state variable, including the total disturbance of the system, $\dot{\psi}_3 = g(t)$, then

$$\begin{cases} \dot{\psi}_1 = \psi_2 \\ \dot{\psi}_2 = \psi_3 + bu \\ \dot{\psi}_3 = g(t) \\ y = \psi_1 \end{cases} \quad (4)$$

The expanded state observer of the system in Eq.4 is:-

$$\begin{cases} \dot{\hat{\psi}}_1 = \hat{\psi}_2 + \beta_1 (\psi_1 - \hat{\psi}_1) \\ \dot{\hat{\psi}}_2 = \hat{\psi}_3 + b_0 u + \beta_2 (\psi_1 - \hat{\psi}_1) \\ \dot{\hat{\psi}}_3 = \beta_3 (\psi_1 - \hat{\psi}_1) \end{cases} \quad (5)$$

where $\hat{\psi}_1$ and $\hat{\psi}_2$ are the estimations of ψ_1 and ψ_2 , respectively. $\hat{\psi}_3$ is the estimation of ψ_3 . β_1 , β_2 and β_3 are selected as $[\beta_1, \beta_2, \beta_3] = [3w_o, 3w_o^2, w_o^3]$ to ensure the stability of the ESO. w_o is the observer bandwidth.

Now, let $\check{\psi}_1 = \psi_1 - \hat{\psi}_1$, $\check{\psi}_2 = \psi_2 - \hat{\psi}_2$ and $\check{\psi}_3 = \psi_3 - \hat{\psi}_3$ the state errors. The estimation errors between Eq.3 and Eq.5 can be indicates as:

$$\begin{cases} \dot{\check{\psi}}_1 = \dot{\psi}_1 - \dot{\hat{\psi}}_1 = -3w_o \check{\psi}_1 + \check{\psi}_2 \\ \dot{\check{\psi}}_2 = \dot{\psi}_2 - \dot{\hat{\psi}}_2 = -3w_o^2 \check{\psi}_1 + \check{\psi}_3 \\ \dot{\check{\psi}}_3 = \dot{\psi}_3 - \dot{\hat{\psi}}_3 = -w_o^3 \check{\psi}_1 + \dot{\psi}_3 \end{cases} \quad (6)$$

Eq.(6) can be written as:

$$\dot{\check{\psi}} = A_e \check{\psi} + B \dot{\psi}_3$$

$$\begin{bmatrix} \dot{\check{\psi}}_1 \\ \dot{\check{\psi}}_2 \\ \dot{\check{\psi}}_3 \end{bmatrix} = \begin{bmatrix} -3w_o & 1 & 0 \\ -3w_o^2 & 0 & 1 \\ -w_o^3 & 0 & 0 \end{bmatrix} \begin{bmatrix} \check{\psi}_1 \\ \check{\psi}_2 \\ \check{\psi}_3 \end{bmatrix} + \begin{bmatrix} 0 \\ 0 \\ \dot{\psi}_3 \end{bmatrix} \quad (7)$$

3.2.2 Fractional ESO

The definition of fractional calculus proposed by Caputo is widely used in fractional order control^[34]. Fractional calculus is a generalization of integration and differentiation to non-integer order operator:-

$$D^{\alpha_f} = \begin{cases} \frac{d^{\alpha_f}}{dt^{\alpha_f}} \text{ for } \alpha_f > 0 \\ 1 \text{ for } \alpha_f = 0 \\ \int_a^t (dt)^{-\alpha_f} \text{ for } \alpha_f < 0 \end{cases} \quad (8)$$

In this approach, only instead of integer order of observer in,Eq.5 using fractional with (α_f) term as shown in Fig. 4.Generally Eq.5 can be rewritten in fractional form as:

$$\begin{aligned} D^{\alpha_f} \hat{\psi}_1 &= \hat{\psi}_2 + \beta_1 (\psi_1 - \hat{\psi}_1) \\ D^{\alpha_f} \hat{\psi}_2 &= \hat{\psi}_3 + b_0 u + \beta_2 (\psi_1 - \hat{\psi}_1) \\ D^{\alpha_f} \hat{\psi}_3 &= \beta_3 (\psi_1 - \hat{\psi}_1) \end{aligned} \quad (9)$$

The fractional term of observer (α_f) can be calculated by any optimization method like, particular swarm optimization (P.S.O), genetic algorithm (G.A)^[35-37].

3.3 linear State Error Feedback (LSEF)

LSEF is the result of a linear combining of state deviations equivalent to TD and ESO^[32].

$$\begin{cases} e_1 = v_1 - \hat{\psi}_1 \\ e_2 = v_2 - \hat{\psi}_2 \\ u_o = k_p e_1 + k_d e_2 \\ u = \frac{u_o - \hat{\psi}_3}{b_0} \end{cases} \quad (10)$$

Where k_p, k_d are proportional and derivative adjustable gains, respectively. The individual moves the shank of the leg while wearing the exoskeleton in our testing. The measured angular position of the exoskeleton is utilized to direct an object toward a fixed target, with a rest position of (-45deg) and a move to (-90deg for flexion) and (0 deg for extension). In this study, we used a linear proportional- derivative controller (LPD) for MADRC .The controller bandwidth (w_c) and damping ratio (ξ) are used to determine the gains (k_p, k_d). These parameters are determined by the design specifications^[38].

$$k_p = \omega_c^2,$$

$$k_d = 2\zeta\omega_c \quad (11)$$

PD controller gains can be calculated according to the analysis from^[38], the bandwidth w_c is related to settling time τ_s of closed-loop system according to the following formula:-

$$w_c = \frac{4}{\tau_s} \quad (12)$$

In this application, the specification of settling time of controlled system is chosen to be $\tau_s = 0.16\text{sec}$ and damping ratio $\zeta = 1$. The observer and PD controller gains can be calculated according to above equation with ($w_c = 25\text{Hz}$). If one chooses the bandwidth of observer ω_o to be equal to $\omega_o = 4\omega_c$. The observer gains ($\beta_1, \beta_2, \beta_3$) values then it easy to calculate.

3.4 Stability analysis of ESO

The "total disturbance" indicated by $f(\psi, w, t)$ is frequently bounded in practice. As a result, $\dot{\psi}_3 = g(t)$ is bounded. Since ($\beta_i > 0$), choosing w_o such that A_e matrix eigenvalues are in the left-hand side, the ADRC system is stable^[39-40], to prove that:-

Since A_e is Hurwitz, there exists a unique positive definite matrix P such that

$$A_e^T P + P A_e = -I \quad (13)$$

Choose the Lyapunov function as:-

$$L = \check{\psi}^T P \check{\psi} \quad (14)$$

The time derivative of Eq.(14) is giving by:-

$$\dot{L} = \dot{\check{\psi}}^T P \check{\psi} + \check{\psi}^T P \dot{\check{\psi}}$$

$$\dot{L} = A_e^T P \check{\psi} + \check{\psi}^T P A_e \check{\psi} + 2B^T P \check{\psi}$$

$$\dot{L} = -\check{\psi}^T I \check{\psi} + 2B^T P \check{\psi}$$

$$\dot{L} \leq -\mu(I) \|\check{\psi}\|^2 + 2\varepsilon \|P\| \|\check{\psi}\|$$

The norm of the state error is limited by after quite a long enough period of time by:-

$$\|\check{\zeta}\| \leq \frac{2\varepsilon \|P\|}{\mu I} \quad (15)$$

where μ is the smallest eigenvalue of a matrix.

Lemma 1. Given a differentiable continuous function $\Upsilon(t)$ satisfying

$$\lambda_1 \leq \Gamma(t) \leq \lambda_2 \quad (16)$$

with positive constant λ_1 and λ_2 . The derivative $\Gamma(t)$ is also bounded.

The estimation error of $\check{\psi}_3$ is bounded, and according to Lemma 1, the derivative of $\check{\psi}_3$ is bounded by:

$$\left| \dot{\check{\psi}}_3 \right| < S \quad (17)$$

Where S is a positive constant.

In general, because A_e is a Hurwitz matrix, the differential equation given by Eq.7 is stable, according to Hurwitz stability theory^[41]. As a result, both ESO of ADRC topologies are stable, and their predicted errors are limited.

4. Result Analysis and Discussion

While the frameworks of both LADRC and FADRC are quite similar, the key variations between them are in the extended state to be evaluated. For the Exoskeleton device, the transient behaviour

and performance evaluation of LADRC and FADRC are explored under two conditions: nominal and disturbances. The results were acquired using a MATLAB simulation.

5.1 Nominal case

On the basis of given sinusoidal signal trajectory with the amplitude of (-45deg or -0.785rad) and the frequency of 0.157 Hz, the simulation are done for the three configuration of ADRC.

5.1.1 LADRC without disturbances

According to Fig.2., the Simulink simulation for the desired trajectory to LADRC is plotted as seen in the Fig. 4., under nominal case(without disturbances).The trajectory tracked by LADRC has reference tracking with (R.M.S.E=0.0033) and small error as shown from trajectory error behaviour.

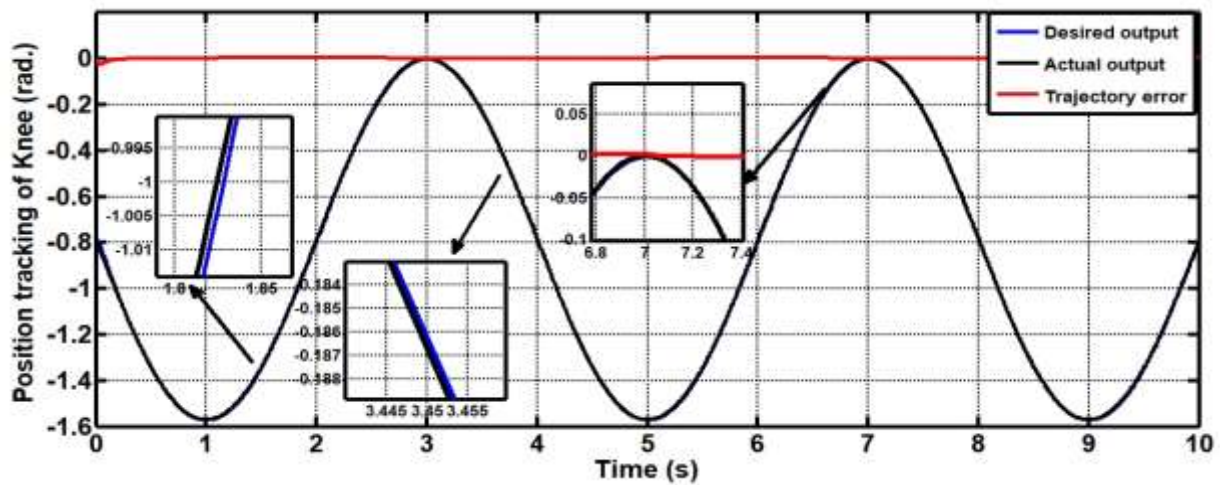


Fig. 4. shows the position of Knee for LADRC controller without disturbance

The key to the success of the ADRC is the ESO, to study the validity of the ESO, we plot $Z3(\hat{\psi}_3)$ for tracking the total disturbances (her the system dynamics).Fig.5. shows that, a good tracking, especially at steady state.

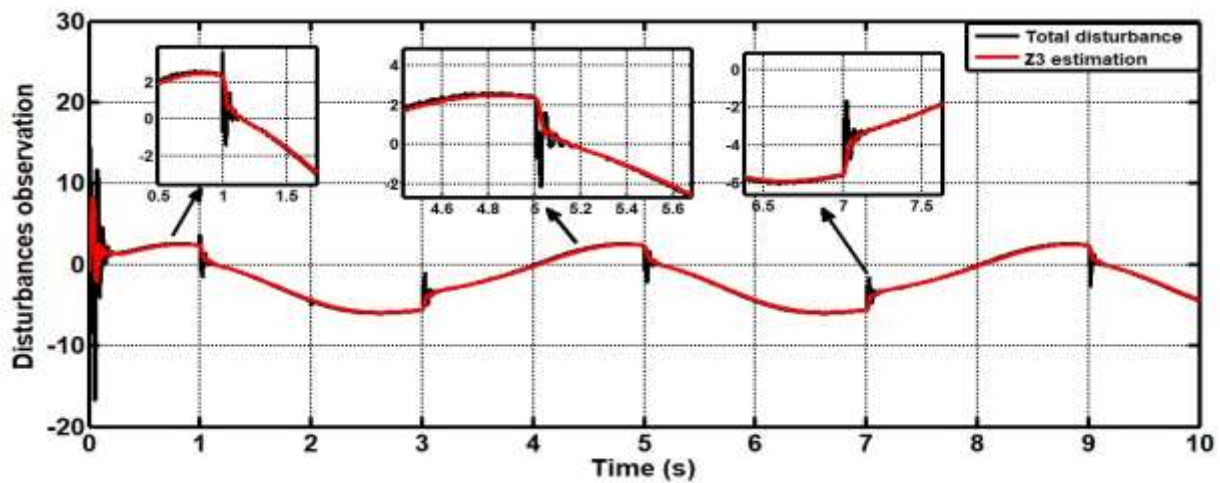


Fig. 5. shows total disturbance and its estimation for LADRC

5.1.2 FADRC without disturbances

According to Fig.3., the Simulink simulation for the desired trajectory to FADRC is plotted as seen in the Fig. 6., under nominal case(without disturbances), The trajectory tracked by FADRC has reference tracking with (R.M.S.E= 0.0026) with small error, when compared with LADRC as shown from trajectory error behaviour.

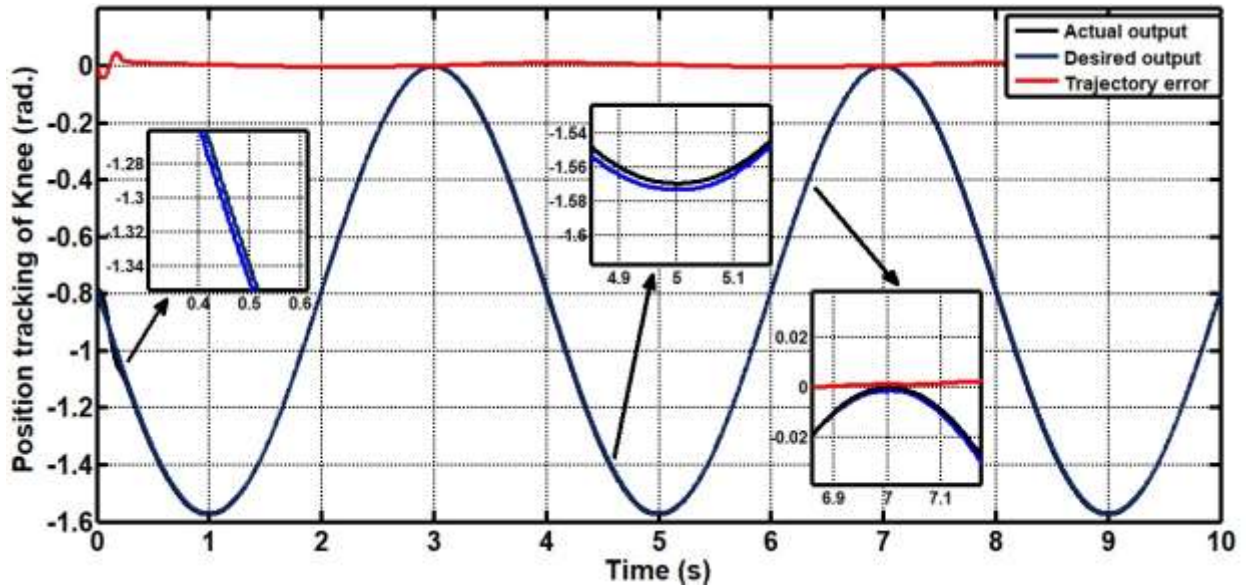


Fig. 6. shows the position of Knee for FADRC controller without disturbance

We plot Z3 for tracking the total disturbances (her the system dynamics).Fig.7. shows that, good tracking, especially at steady state.

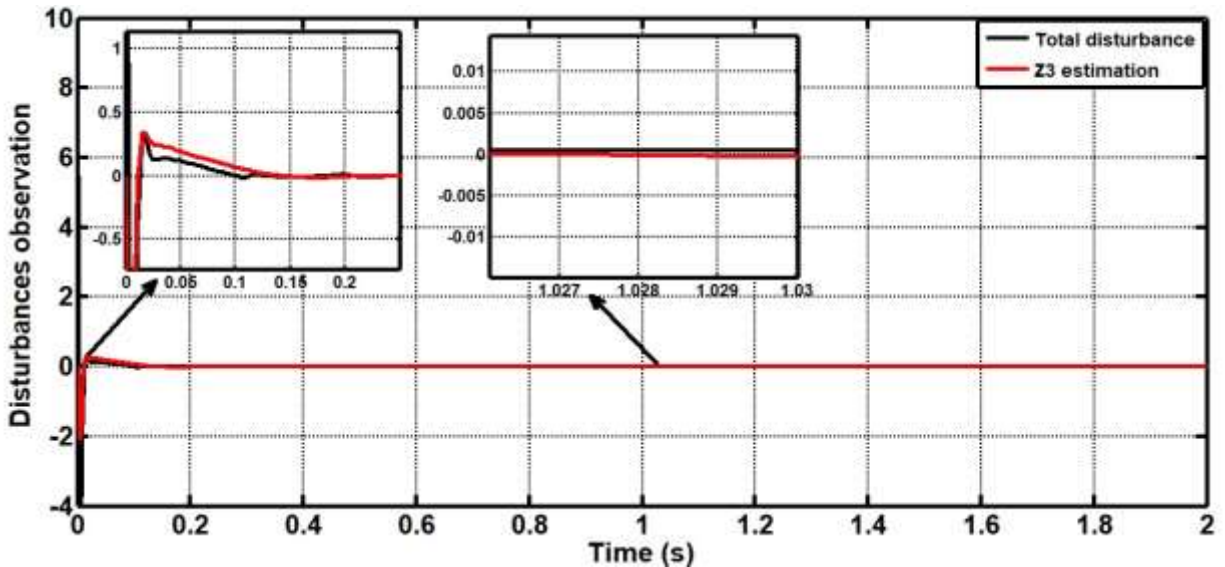


Fig. 7. shows total disturbance and its estimation for FADRC

5.2 Constant torque disturbance

During the test, we illustrate the reliability of the suggested control techniques against a limited load disturbances at the output. The performance of the suggested controllers are compared to theirs in terms of disturbance rejection. An external individual has been forced to apply a resistive torque (disturbance) to the subject's shank for a short period of time (torque load=0.25N.m and time=2sec).

5.2.1 LADRC with disturbances

According to Fig.3., the Simulink simulation for the desired trajectory to LADRC is plotted as seen in the Fig. 8., under disturbance case, The trajectory tracked by LADRC has reference tracking with (R.M.S.E= 0.0269) as shown from trajectory error behaviour.

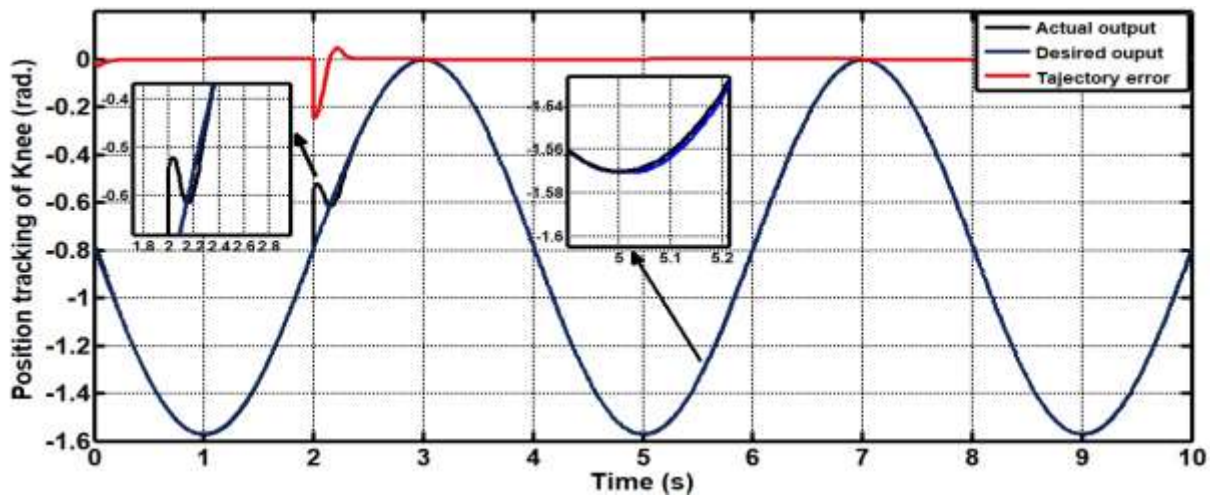


Fig. 8. shows the position of Knee for LADRC controller with disturbance

We plot Z3 for tracking the total disturbances (her the system dynamics with load disturbance).Fig.9. shows that, good tracking, especially at steady state.

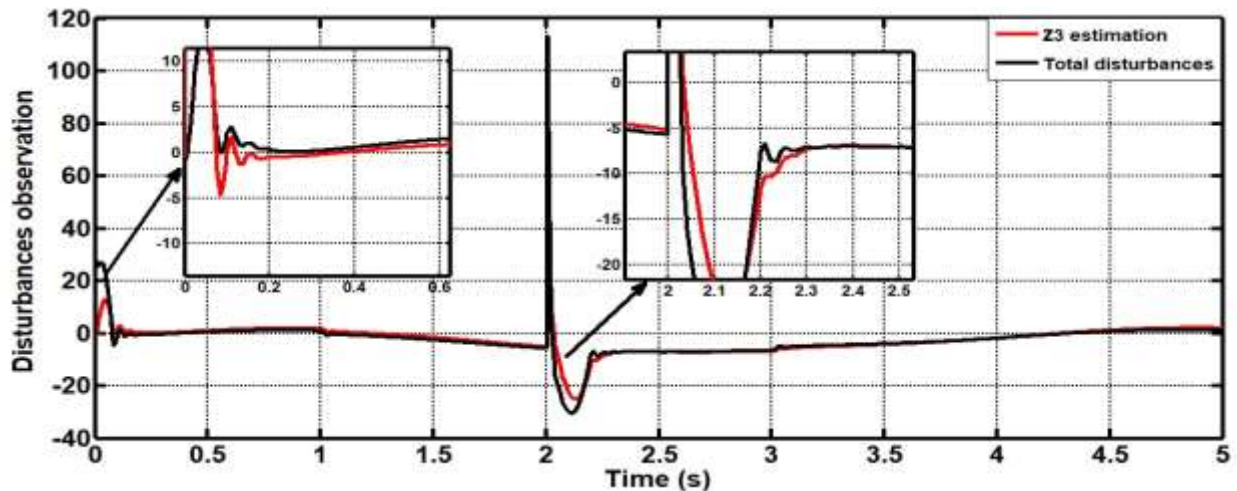


Fig. 9. shows total disturbance and its estimation for LADRC with disturbance

5.2.2 FADRC with disturbances

The Simulink simulation for the desired trajectory to FADRC is plotted as seen in the Fig. 10., under disturbances case, The trajectory tracked by FADRC has reference tracking with (R.M.S.E= 0.0241) with small error, when compared with LADRC as shown from trajectory error behaviour.

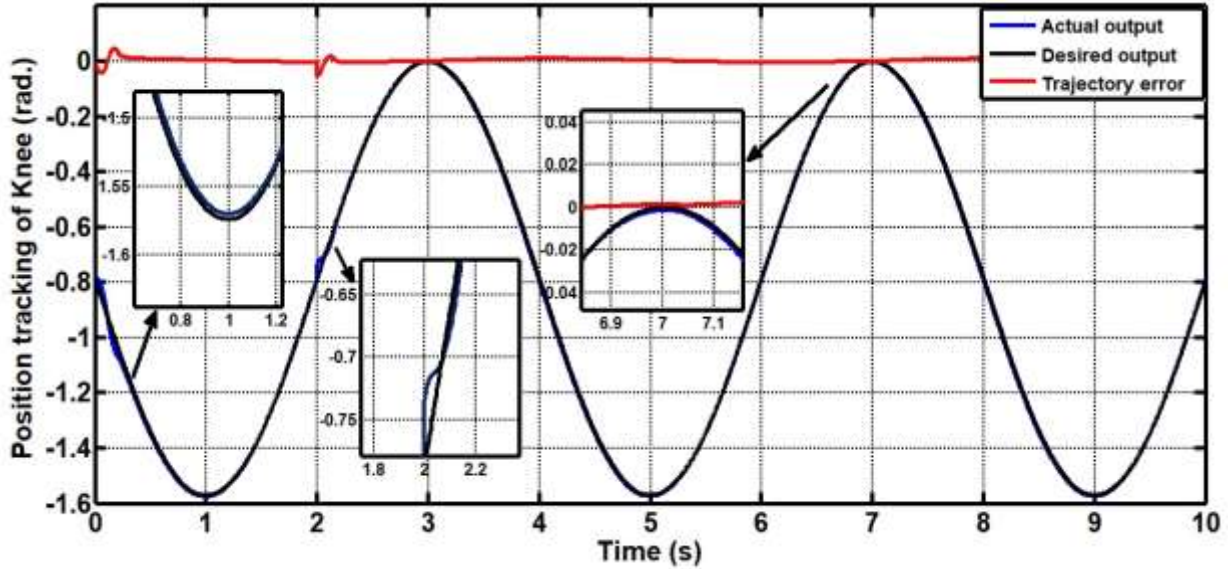


Fig. 10. shows the position of Knee for FADRC controller with disturbance

We plot Z3 for tracking the total disturbances with load disturbance. Fig.11. shows that, good tracking, especially at steady state

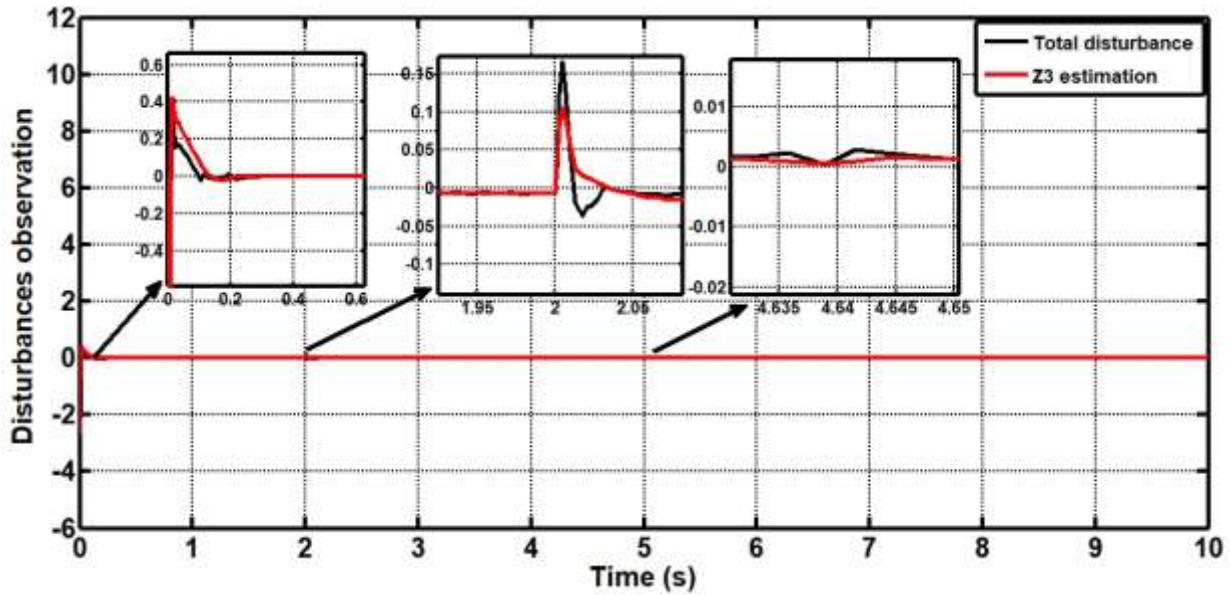


Fig. 11. shows total disturbance and its estimation for FADRC with disturbance

5.3 Noise disturbance case

During the test, we illustrate the reliability of the suggested control techniques against a Gaussian noise was applied with variance equal to (10^{-5}) and zero mean at the output. The performance of the suggested controllers are compared to theirs in terms of disturbance rejection. This section focuses on the effect of the noise

5.3.1 LADRC with disturbance

The Simulink simulation for the required trajectory to LADRC is presented in Fig. 12. under Gaussian white disturbance scenario to evaluate the antidisturbance effectiveness of the LADRC. The output response was dramatically influenced by applying amount of noise to the measured output. The dynamic performance of the controller can be shown to have certain variations for antidisturbance. As can be seen from the trajectory error behavior, the trajectory tracked by LADRC has reference tracking (R.M.S.E=0.0582).

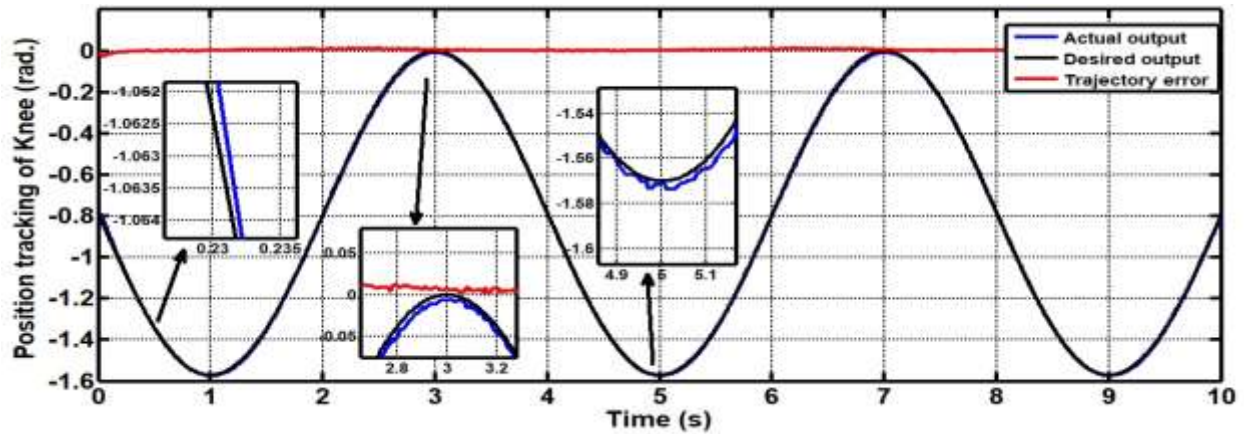


Fig. 12. shows the position of Knee for LADRC controller with Gaussian noise disturbance

We plot Z3 for tracking the total disturbances with noise disturbance. Fig.13. shows that with more fluctuations due to adding Gaussian noise disturbance, but in general there is acceptable tracking between total disturbances and the estimation extra state Z3.

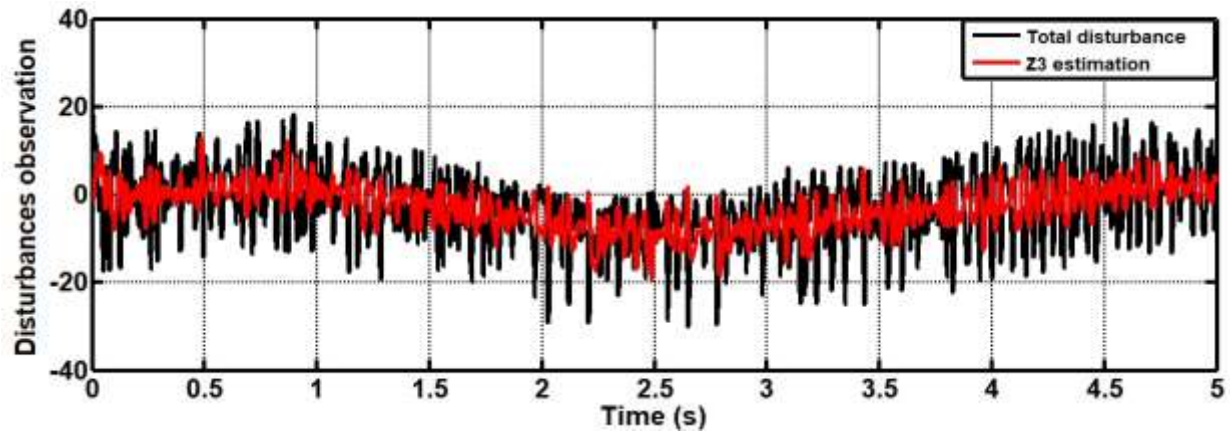


Fig. 13. shows total disturbances and its estimation for LADRC with noise disturbance

5.3.2 FADRC with disturbance

To test the antidisturbance efficiency of the FADRC, a Simulink simulation for the required path to FADRC is shown in Fig. 14. under a Gaussian white disturbance scenario. The quantity of noise applied to the measured output seemed to have a small impact on the output response, when compared to LADRC behaviour. The controller's dynamic performance can be proven to have specific antidisturbance variations. The trajectory tracked by FADRC has reference tracking (R.M.S.E=0.0329), as can be observed from the trajectory error behavior.

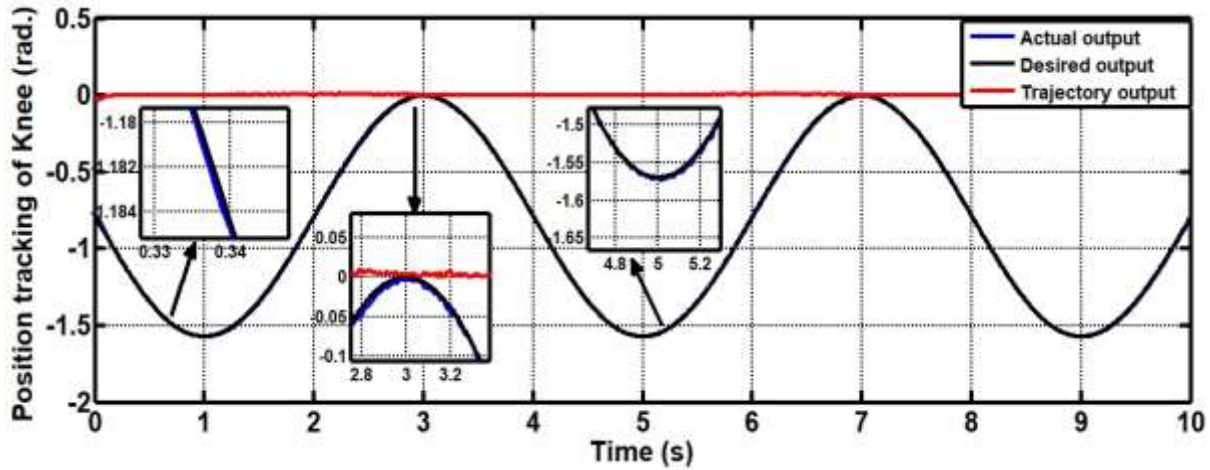


Fig. 14. shows the position of Knee for FADRC controller with Gaussian noise disturbance

For tracking total disturbances with noise disturbance, we plot Z3, as shown in Fig.15., overall tracking between total disturbances and the estimation extra state Z3 is satisfactory, when compared with LADRC.

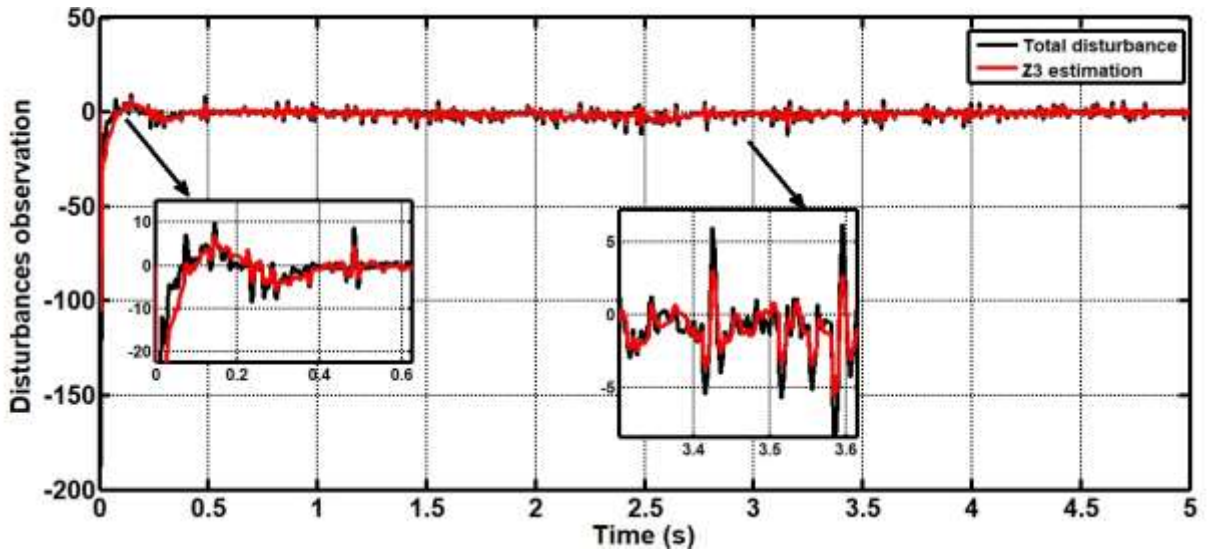


Fig. 15. shows total disturbances and its estimation for FADRC with noise disturbance

For comparison between all configurations of ADRC as appear in the figures and Table 2 with based on performance index (R.M.S.E), the FADRC approach performs better and tracks the

trajectory more efficiently, Despite the fact that the FADRC seems to have some drawbacks over the CADRC, such as the design becoming more complicated and the range of optimal values expanding as a result of the fractional term, the FADRC has several advantages over the LADRC.

Table 2. Numerical report of disturbance rejection capability

Controller Types	R.M.S.E without disturbance	R.M.S.E with constant disturbance	R.M.S.E with noise disturbance
LADRC	0.0033	0.0269	0.0582
FADRC	0.0026	0.0241	0.0329

5. Conclusions

The design and analysis of two methods LADRC and FADRC for exoskeleton device position control are discussed in this study. The effectiveness of all controllers is measured in terms of their ability to reject disturbances. Each of the suggested controller structures has a number of design characteristics that must be fine-tuned before the control. G.A is the recommended tuner in charge of optimization for finding the fractional terms (α_f). Simulated results show that the position response of the knee joint based on FADRC is faster with lower R.M.S.E than that based on LADRC in the nominal situation. It has been observed that the FADRC has stronger disturbance rejection capabilities than the LADRC in the disturbance case, when a disturbing force of constant load is introduced during the training cycle. It show that the tracking of extra state (Z3) is very closely to total disturbance in FADRC and this case appear that FESO of FADRC is very active,when compared with LESO of LADRC because ESO is reconstructed as a fractional one, and the resulting modified fractional extended states observer (FESO) accurately estimates both the overall disturbance and the fractional order dynamic states, resulting in a smaller observer bandwidth. Generally the simulation findings demonstrate that FADRC has higher inherent superiority and potential for tracking control and disturbance rejection.

In the future, the proposed ADRCs can be employed for two degrees of freedom (knee and hip) to improve tracking, as well as different optimization approaches such as Particle Swarm Optimization (PSO), Differential Evolution (DE), and others can be used. The uncertainty case, in which the values of the exoskeleton device are allowed to vary from their nominal values, can also be taken into account.

Declarations

Availability of data and materials

The datasets generated during the current study are available in the references section:-

[31]Saber, M., Djamel, E.C. (2019). A robust control scheme based on sliding mode observer to drive a knee-exoskeleton. *Asian Journal of Control*, 21(1),439-455.
<https://doi.org/10.1002/asjc.1950>

Competing interests

The authors declare no competing financial interests.

Funding

Supported by the Foundation of Control and System Engineering (University of Technology), Ministry of Education.

Authors contributions

N A. conceived the basic idea, and carried out research, analysis and writing of the manuscript. A J. provided theoretical guidance. A S. assisted with formula analyses. N A. was in charge of drawing figures. A J. and A S. revised the final manuscript. All authors read and approved the final manuscript.

Acknowledgements

The authors would like to thank the control and system engineering department for its support in the present work.

References

[1] Baud R.M and Ijspeert A.R. (2021). Review of control strategies for lower-limb exoskeletons to assist gait. *J NeuroEngineering Rehabil*, 18(119).
<https://doi.org/10.1186/s12984-021-00906-3>

[2] Emken J.L., Harkema S.J., Beres-Jones J.A., Ferreira C.K.Reinkensmeyer D.J.(2007). Feasibility of manual teach-and-replay and continuous impedance shaping for robotic locomotors training following spinal cord injury. *IEEE Trans. Biomed. Eng.* 55: 322-334.
<https://doi.org/10.1109/TBME.2007.910683>

[3] Su, Y., Sun D., Ren L., Mills J.K.(2006). Integration of saturated PI synchronous control and PD feedback for control of parallel manipulators. *IEEE Trans. on Robot.* 22: 202-207
<https://doi.org/10.1109/TRO.2005.858852>

- [4] Jamwal, P.K., Xie, S.Q., Hussain, S., Parsons, J.G. (2012). An adaptive wearable parallel robot for the treatment of ankle injuries. *IEEE/ASME Trans. Mechatronics* 19: 64-75
<https://doi.org/10.1109/TMECH.2012.2219065>
- [5] Kazerooni, H., Racine, J.L., Huang, L., Steger, R. (2005). On the control of the berkeley lower extremity exoskeleton (BLEEX). *In Proceedings of the 2005 IEEE international conference on robotics and automation*, Barcelona, Spain, 18-22 April: 4353-4360.
- [6] Taha, Z., Majeed, A.P.A., Abidin, A.F.Z., Ali, M.A.H., Khairuddin, I.M., Deboucha, A., Tze, M.Y.W.P. A.(2018).hybrid active force control of a lower limb exoskeleton for gait rehabilitation. *Biomed. Tech. Eng.* 63: 491-500.
<https://doi.org/10.1515/bmt-2016-0039>
- [7] Yang, Z., Zhu, Y., Yang, X., Zhang, Y. (2009). Impedance control of exoskeleton suit based on adaptive RBF neural network. *In Proceedings of the 2009 International Conference on Intelligent Human-Machine Systems and Cybernetics*, China,1:182-187.
<https://doi.org/10.1109/IHMISC.2009.54>
- [8] Li, S., Yang, J., Chen, W.H., Chen, X. (2016). Disturbance observer-based control: methods and applications. *In Proceedings of the 2016 International Conference on Unmanned Aircraft Systems (ICUAS)*, USA: 7-10.
<https://doi.org/10.1201/b16570>
- [9] Lu, R., Li, Z., Su, C.Y., Xue, A. (2013). Development and learning control of a human limb with a rehabilitation exoskeleton. *IEEE Trans. Ind. Electron.* 61: 3776-3785.
<https://doi.org/10.1109/TIE.2013.2275903>
- [10] Gao, Z., Huang, Y., Han, J. (2001). An alternative paradigm for control system design. *In Proceedings of the 40th IEEE Conference on Decision and Control*, Orlando, USA,5: 4578-4585.
- [11] Zhu, E., Pang, J., Sun, N., Gao, H., Sun, Q., Chen, Z.(2013). Airship horizontal trajectory tracking control based on Active Disturbance Rejection Control (ADRC). *Nonlinear Dyn.* 75: 725-734.
<https://doi.org/10.1007/s11071-013-1099-x>
- [12] Desai, R., Patre, B.M., Pawar, S.N. (2018). Active disturbance rejection control with adaptive rate limitation for process control application. *In Proceedings of the 2018 Indian Control Conference (ICC)*, India: 131-136.
<https://doi.org/10.1109/INDIANCC.2018.8307966>
- [13] Dulf, E.H., Both, R., Muresan, C.I. (2014). Active disturbance rejection controller for a separation column. *In Proceedings of the 2014 IEEE International Conference on Automation*,

Quality and Testing, Robotics, Romania: 1-6.
<https://doi.org/10.1109/AQTR.2014.6857906>

[14] Amjad, J. H., Hussein, M. B., Akram, H.H. (2018). PSO-Based Active Disturbance Rejection Control for Position Control of Magnetic Levitation System. *2018 5th International Conference on Control, Decision and Information Technologies*, Greece 1:8.

[15] Wameedh, R.A., Ibraheem, K.I., Amjad, J. H. (2021). Model-free active input-output feedback linearization of a single-link flexible joint manipulator: An improved active disturbance rejection control approach. *Measurement and Control*. 54: 856-871.
<https://doi.org/10.1177/0020294020917171>

[16] Garran, P.T., Garcia, G. (2017). Design of an optimal PID controller for a coupled tanks system employing ADRC. *IEEE Lat. Am. Trans.* 15: 189-196
<https://doi.org/10.1109/TLA.2017.7854611>

[17] Li, D., Ding, P., Gao, Z. (2016). Fractional active disturbance rejection control. *ISA Trans.* 62:109-119.
<https://doi.org/10.1016/j.isatra.2016.01.022>

[18] Gao, Z. (2006). Active disturbance rejection control: A paradigm shift in feedback control system design. *In Proceedings of the American Control Conference*, USA: 2399-2405.

[19] Madonski, R., Shao, S., Zhang, S., Gao, Z., Yang, J., Lia, S. (2019). General error-based active disturbance rejection control for swift industrial implementations. *Control Engineering Practice*, 84:218-229.
<https://doi.org/10.1016/j.conengprac.2018.11.021>

[20] Marcin, N., Rafał, M., Krzysztof, K. (2015). First look at conditions on applicability of ADRC. *International Workshop on Robot Motion and Control Conference*, Poland: 1-7.

[21] Widhi, Y.S., Adha, I.C. (2016). Modeling and Design of Low Cost Lower Limb Rehabilitation Robot Control System for Post Stroke Patient using PWM Controller. *International Journal of Mechanical & Mechatronics Engineering*, 16(1):101-108.

[22] Zhijian, H., Yudong, L., Yihua, L., Wenbo, S., Guichen, Z. (2018). An ADRC Method for Noncascaded Integral Systems Based on Algebraic Substitution Method and Its Structure. *Mathematical Problems in Engineering*, 1-10.
<https://doi.org/10.1155/2018/3905879>

[23] Laura, M.C., David, J. R. (2009). Review of control strategies for robotic movement training after neurologic injury. *Journal of NeuroEngineering and Rehabilitation*, 6(20):1-15.
<https://doi.org/10.1186/1743-0003-6-20>

- [24] Miao, Q., Zhang, M., Cao, J. (2018). Reviewing high-level control techniques on robot-assisted upper-limb rehabilitation. *Advanced Robotics*, 32(24), 1253-1268.
<https://doi.org/10.1080/01691864.2018.1546617>
- [25] Gao,Z.(2003).Scaling and Parameterization Based Controller Tuning. *Proc. of the American Control Conference*, 4989-4996.
- [26] Dazi Li , Pan Ding , Zhiqiang Gao.(2016). Fractional active disturbance rejection control. *ISA Transactions* ,62, 109-119.
<https://doi.org/10.1016/j.isatra.2016.01.022>
- [27] Song, J., Lin, J., Wang, L., Wang, X., and Guo, X. (2017).Nonlinear FOPID and active disturbance rejection hypersonic vehicle control based on DEM biogeography-based optimization. *Journal of Aerospace Engineering*, 30, 04017079
[https://doi.org/10.1061/\(ASCE\)AS.1943-5525.0000786](https://doi.org/10.1061/(ASCE)AS.1943-5525.0000786)
- [28] Zhou, X., Yang, C., Zhao, B., Zhao, L., and Zhu, Z. (2018).A high-precision control scheme based on active disturbance rejection control for a three-axis inertially stabilized platform for aerial remote sensing applications. *Journal of Sensors*, 7295852
<https://doi.org/10.1155/2018/7295852>
- [29] Chen, P., Luo, Y., Zheng, W., and Gao, Z. (2019).A New Active Disturbance Rejection Controller Design Based on Fractional Extended State Observer. *Chinese Control Conference (CCC).IEEE*, 4276-4281.
<https://doi.org/10.23919/ChiCC.2019.8865339>
- [30] Fang, H., Yuan, X., and Liu, P.(2018).Active-disturbance-rejection-control and fractional-order-proportional-integral-derivative hybrid control for hydroturbine speed governor system. *Measurement and Control*. 51, 192-201.
<https://doi.org/10.1177/0020294018778312>
- [31] Saber, M.; Djamel, E.C. (2019). A robust control scheme based on sliding mode observer to drive a knee-exoskeleton. *Asian Journal of Control*, 21(1),439-455.
<https://doi.org/10.1002/asjc.1950>
- [32] Han, J. (2009).From PID to active disturbance rejection control. *IEEE Transactions on Industrial Electronics*,56(3),900-906.
<https://doi.org/10.1109/TIE.2008.2011621>
- [33] Wameedh, R.; Ibraheem, K.; Amjad, J. (2020). Novel Active Disturbance Rejection Control Based on Nested Linear Extended State Observers. *Appl. Sci.*, 10,1-27.
<https://doi.org/10.3390/app10124069>

[34] E. Oliveira¹, J. Machado.(2014).A Review of Definitions for Fractional Derivatives and Integral. *Mathematical Problems in Engineering*.1-6.
<https://doi.org/10.1155/2014/238459>

[35] Cheng, P., Yantao, T., Yue, B., Xun, G., Changjun, Z., Qingjia, G .(2013). ADRC Trajectory Tracking Control Based on PSO Algorithm for a Quad-Rotor.*IEEE 8th Conference on Industrial Electronics and Applications (ICIEA)*,800-805.
<https://doi.org/10.1109/ICIEA.2013.6566476>

[36] Zhou, X., Gao, H., Zhao, B.,Zhao, L. (2018). A GA-based parameters tuning method for an ADRC controller of ISP for aerial remote sensing applications.*ISA Transactions*, 1-31.
<https://doi.org/10.1016/j.isatra.2018.08.001>

[37] Katoch S., Chauhan S.S., Kumar V .(2021) A review on genetic algorithm: past, present, and future. *Multimed Tools Appl* ,80, 8091-8126.
<https://doi.org/10.1007/s11042-020-10139-6>

[38] Chen, X., D. Li, Z. Gao. (2011).Tuning method for second-order active disturbance rejection control. *Chinese Control Conference*, IEEE,6322-6327.

[39] Zhang,Q., Gao,L., Gao,Z.(2007).On stability analysis of active disturbance rejection control for nonlinear time-varying plants with unknown dynamics. *In Proceedings of IEEE conference on Decision and Control*. 3501-3506.

[40] Zheng,Q.,Chen,Z.,Gao,Z.(2009).A practical approach to disturbance decoupling control. *Control Engineering Practice*, 17(9),1016-1025.
<https://doi.org/10.1016/j.conengprac.2009.03.005>

[41] Zhang,W.,Shen,S., Han,Z.(2008).Sufficient conditions for Hurwitz stability of matrices. *Latin American applied research*, 38(3), 253-258.